

# Graph Cuts Segmentation Approach Using a Patch-Based Similarity Measure Applied for Interactive CT Lung Image Segmentation

Aicha Majda, Abdelhamid El Hassani

**Abstract**—Lung CT image segmentation is a prerequisite in lung CT image analysis. Most of the conventional methods need a post-processing to deal with the abnormal lung CT scans such as lung nodules or other lesions. The simplest similarity measure in the standard Graph Cuts Algorithm consists of directly comparing the pixel values of the two neighboring regions, which is not accurate because this kind of metrics is extremely sensitive to minor transformations such as noise or other artifacts problems. In this work, we propose an improved version of the standard graph cuts algorithm based on the Patch-Based similarity metric. The boundary penalty term in the graph cut algorithm is defined Based on Patch-Based similarity measurement instead of the simple intensity measurement in the standard method. The weights between each pixel and its neighboring pixels are Based on the obtained new term. The graph is then created using these weights between its nodes. Finally, the segmentation is completed with the minimum cut/Max-Flow algorithm. Experimental results show that the proposed method is very accurate and efficient, and can directly provide explicit lung regions without any post-processing operations compared to the standard method.

**Keywords**—Graph cuts, lung CT scan, lung parenchyma segmentation, patch based similarity metric.

## I. INTRODUCTION

LUNG diseases are one of the most important and significant health care challenges in the world. According to American Thoracic Society, hundreds of millions of peoples in the worldwide are affected by lung diseases such as Chronic Obstructive Pulmonary Disease (COPD), Asthma, Tuberculosis, and the Lung Cancer which causes around 1.69 million of deaths yearly [1].

Most patients with lung disease such lung cancer, are diagnosed when they have an advanced stage disease, they present with symptoms, making curative treatment no longer a solution. In this context, an effective screening test is needed for early detection with the aim of reducing the mortality rate. With the advancement of screening technologies, Computed Tomography (CT) scan was shown to be a potential screening test for such cases [2].

An accurate Segmentation method is a key role for quantitative lung computed (CT) image analysis and also for computer-aided diagnosis [3] which helps the physician in both screening utilities and clinical decision [2]. Lung parenchyma segmentation is a prerequisite for lung CT image processing. It consists of selecting pulmonary tissue in the

CT slices so that the CAD system that detects or quantify pathologies for lung diseases can be applied more accurately to measure or to analyze the target object.

Until recently, a large number of Lung Segmentation approaches [4]-[6] have been proposed in the literature. Many methods appear to be simple and effective. They rely on the contrast information where a normal lung appears dark in a CT image while it is surrounded by denser regions [7]. It is a simple and an effective idea, but it fails when the extraction concerns pathological lung tissues, particularly when the lesion is attached to the pleura of the lung such as juxta-pleural nodules.

Also, these methods are most likely to follow a post-processing to remove the main bronchus or to reduce the false positive rate in the segmentation result. Therefore, most lung segmentation methods currently use post-processing methods that are based on gray level thresholding [8], [9] combined with other extraction methods.

In this work, we propose a lung segmentation approach Based on graph cuts [10], [11] as a powerful optimization technique to get the optimal segmentation. The graph cuts framework was first proposed by Boykov [12] to obtain globally optimal object segmentation in N-dimensions. Since then, the graph cuts has received an increasing attention and been quickly developed and applied in a wide range of research [13], [14], [10].

In [15], Nakagomi et al. proposed an extended version of the graph cuts algorithm, applied for the lung segmentation with pleural effusion. The energy function is extended with multiple-shapes and neighbor structure constraints, which gave a high rate of segmentation accuracy.

In [16], Dai et al. proposed an improved graph cuts algorithm based on a Gaussian Mixture Model (GMM), in which the weight that each pixel belongs to the foreground or the background object is obtained using the Expectation-Maximization (EM) algorithm.

In this paper, our presented work proposes an improved version of the standard graph cuts algorithm based on the Patch-Based similarity metric to express the boundary term instead of an ad-hoc function as used in the previous works [12], [16]. The weight connecting each pixel to its neighboring pixels is then computed using the new formula of the boundary term. Our proposed method achieves an accurate segmentation (with a 0.9406 Dice-Coefficient index) using only the energy function without any post-processing methods.

In Section II, the Patch-Based similarity metric and the

graph Cuts algorithm are summarized. Then, the proposed method is detailed in Section III. In Section IV, we compare our proposed Method with the standard graph Cuts using the well known LIDC database [17], [18] under different CT lung image cases. In the last Section V, concluding remarks are stated.

## II. METHODS

In this section, Our Lung CT segmentation approach is described in detail. But first, we give the basic definition of the Graph Cuts and a brief view of the patch Based similarity measure respectively in Subsections II.A and II.B. Then our segmentation process is detailed in the next following Section III.

### A. Patch-Based Similarity Measure

In [19] Buades et al. proposed an efficient image processing algorithm applied for image denoising [20] called Non-Local Means (NLM). The NLM stems from the assumption that each small structure element, in a given natural image, has many similar small structures in the same image.

Following this insight, the NLM algorithm restore the corrupted values of noisy pixels by averaging the intensity values of all pixels in the image whose neighborhoods are similar to the neighborhood of the target pixel.

In a previous work [21], we have given a full description of the NLM algorithm and its applications in medical image analysis.

The NLM uses a patch based similarity measure denoted  $w(p, q)$  which is the weight depending on the similarity between two pixels  $p$  and  $q$ , and satisfies the conditions  $w(p, q) \in [0, 1]$  and  $\sum w(p, q) = 1$ . The weight is expressed as follows:

$$w(p, q) = \frac{1}{Z(p)} e^{-\frac{d(p,q)}{h^2}} \quad (1)$$

where  $h$  is the smoothing parameter and  $Z(p)$  is the normalizing constant to ensure that  $w(p, q)$  sums up to one.  $N_p$  and  $N_q$  are respectively two patches of size  $k \times k$  ( $k = 2 \times r_k + 1$ , where  $r_k$  is the radius) and centered at  $p$  and  $q$ .  $d(p, q)$  is the similarity Euclidean distance between the  $N_p$  and the patch  $N_q$ .

$$d(p, q) = G_f \|A_p(N_p) - A_q(N_q)\|_2^2 \quad (2)$$

where  $G_f$  is a normalized Gaussian weighting function.  $A_p$  and  $A_q$  are respectively the  $p$  and  $q$  intensity values

In this work, we use the patch-based similarity measure described in the NLM algorithm to introduce the weights term that represents pixel-similarity as a boundary term in the Graph Cuts Algorithm. In fact, the similarity between neighbors will be not depending on the intensity value as much as it depends on the image structure. The detailed explanation of the boundary term is expressed in the following section.

### B. Graph Cuts

As mentioned previously, The graph cuts approach has been widely applied as a global optimization method for image segmentation problems. The image represented using an adjacency graph that is set up such that every pixel in the image is represented by a node in the graph [16]. Each pixel is connected to its neighboring pixels with a specific edge, given a cost that is weighted by the difference in the pixel intensities. Two additional nodes added to the graph called the Source and the Sink node. These two nodes represent the foreground region and background region respectively. Each pixel in the image; which is represented by a node in the graph; is connected to the aforementioned two nodes: Source and Sink. the cost of these two connections is applied according to the probability that the connected pixels intensity occurs in the foreground or the background distribution.

Once the graph is set up, the min-cut/max-flow algorithm [22] is performed to search for the optimal Cut that separate the Source node from the Sink node, which means separate the foreground from the background region. Detailed informations on the Graph Cuts can be found in [12].

The optimization or minimum cut criterion is defined as:

$$\text{mincut}\{C1, C2\} = \sum_{e \in C} (\omega(e)) \quad (3)$$

where  $C = \{C1, C2\}$  is a cut and  $w$  is the weight (cost) of the edges connecting C1 to C2. Considering an arbitrary set of data elements P and some neighborhood system represented by a set N of all unordered pairs of pixels p,q, let  $A = \{A_1, A_2, \dots, A_p\}$  be a binary vector of labels and A is the label F or B for the pixel p. Vector A defines a segmentation and can represent either the foreground object or background. Therefore, the energy function E(A) for segmentation is defined as in [12] as follows:

$$E(A) = \lambda R(A) + B(A); \quad (4)$$

where:

$$R(A) = \sum_{p \in P} (R_p(A_p)) \quad (5)$$

$$B(A) = \sum_{(p,q) \in N} B_{(p,q)} \cdot \delta(A_p, A_q) \quad (6)$$

$$\delta(A_p, A_q) = \begin{cases} 1 & A_p \neq A_q \\ 0 & \text{otherwise} \end{cases} \quad (7)$$

where  $R(A)$  is a regional properties term, which assumes that the individual penalties for assigning pixel p to "obj" or "bkg" correspondingly penalty are  $R_p$ ("obj") or  $R_p$ ("bkg").  $B(A)$  is the boundary properties term that comprises the boundary properties of segmentation A. The coefficient  $\lambda \geq 0$  in (4) specifies a relative importance of  $R(A)$  versus  $B(A)$ .

$$R_p(A = 1) = -\ln(\Pr(A_p | \text{"obj"})) \quad (8)$$

$$R_p(A = 0) = -\ln(\Pr(A_p | \text{"bkg"})) \quad (9)$$

where "obj" and "bkg" are the sets of pixels marked manually object (obj) regions and background (bkg) regions and A is the

TABLE I  
 DICE'S COEFFICIENT INDEX

-	Graph Cuts	Proposed Method
$\ R_{seg} \cap R_{Gt}\ $	$\approx 3.8 \times 10^4$	$\approx 3.9 \times 10^4$
$\ R_{seg}\  \oplus \ R_{Gt}\ $	$\approx 9.1 \times 10^4$	$\approx 8.3 \times 10^4$
DSC	0.8398	0.9406

intensity of pixel  $p$ . The User interaction is needed to provide  $obj$  and  $bkg$ . The boundary term [16] commonly used is:

$$B_{p,q} \propto \exp\left(-\frac{(A_p - A_q)^2}{2\sigma^2}\right) \frac{1}{dist(p,q)} \quad (10)$$

where  $dist(p,q)$  is the Euclidean distance between pixels  $p$  and  $q$  in the image coordinate and  $\sigma$  is a parameter that can be chosen empirically.

Finally, In the graph cuts algorithm, the user needs to choose the seed points for the foreground region (denoted  $obj$ ) and the background region (denoted  $bkg$ ) in the image to specify which part of the image represents the target {foreground / Background}. Further details about the seed points and the weight of their edges can be found in [12].

### III. PROPOSED SEGMENTATION METHOD

As mentioned in the previous section, the second term  $B_{p,q}$  (which is the boundary term) expresses the penalty for assigning labels  $A_p$  and  $A_q$  to the two neighboring pixels  $p$  and  $q$ .

The computation formula is based originally on the two-pixel intensities and the distance between them. In case of 4-connected neighborhood pixel connectivity, the term is controlled only by the intensity distance between the two pixels. Then, as mentioned previously, the weight between the two pixels is high when the intensity distance between them is too small.

Although, the term is shown to be effective in multiple segmentation studies, it fails to handle an abnormal Lung Segmentation problem, without following post-processing steps. In the case of an abnormal Lung segmentation, the term should give a high weight for two pixels which one of them is located in the lung parenchyma while the other is located in a nodule region or a blood vessel, even if their intensities are different. In order to improve the boundary term, we propose to use the Patch-Based Similarity Measure as described in (1) instead of the simple Intensity-Based similarity term, to take into account the structure similarity during the measurement. The new boundary term is expressed as follows:

$$B_{p,q} \propto \frac{1}{Z(p)} \cdot \exp\left(-\frac{G_p \|A(N_p) - A(N_q)\|_2^2}{h^2}\right) \quad (11)$$

$Z(p)$  is the sum of all weights between the pixel  $p$  and each pixel  $k$  belong to the volume search window centered at the pixel  $p$ :

$$Z(p) = \sum_{k \in V_p} B_{p,k} \quad (12)$$

### IV. EXPERIMENTS & RESULTS

To report our experimental results, we adopted CT lung images [17] from The Lung Image Database Consortium image collection (LIDC-IDRI) that consists of diagnosing and lung cancer screening thoracic CT scans with marked-up annotated lesions [23]. It is a web-accessible resource for development, training, and evaluation of CAD methods [18] for lung cancer detection and diagnosis.

We compare our proposed method with the Standard Graph Cuts Method. Comparison with the standard Graph Cuts with other conventional methods can be found in great detail in [24], [15].

In the following experiment, we use a random patient data from the LDIC database, with a volume size =  $512 \times 512 \times 111$ . Firstly, we separate the images into two regions: the information area and the empty area in the Target CT lung image. These two areas don't represent the foreground and the background in the aforementioned sections. Simply, we want to remove the information that doesn't belong to the area of study.

In a previous work, we have demonstrated how to accurately separate those two regions using a dynamic structuring element with a non-fixed shape with stepwise morphological operations [21].

This first pre-process is performed with the idea in mind that our proposed segmentation approach will be applied only on the information area (called  $\mathcal{O}$  for simplicity), while we skip any process related to the empty area (called  $\mathcal{B}$  for simplicity) since each one of its pixels is labeled. Results of this first pre-process is shown in Fig. 2.

It should be noted that the  $\mathcal{O}$  and  $\mathcal{B}$  are different from the previously mentioned  $obj$  and  $bkg$ .

To evaluate the performance of our segmentation approach, we use the Dice Coefficient Index as a similarity measurement to quantify the consistency between the segmented results (denoted  $R_{seg}$ ) and the Ground Truth of the Lung Parenchyma (denoted  $R_{Gt}$ ) provided by a manual Segmentation (performed by our Team's Radiologist). The Dice coefficient index is given by:

$$DSC = 2 \cdot \frac{\|R_{seg} \cap R_{Gt}\|}{\|R_{seg}\| \oplus \|R_{Gt}\|} \quad (13)$$

Table I represents the mean value of the Dice coefficient index for all tested cases. We have compared our proposed method with the standard Graph-Cuts Method. Comparison of the standard Graph-Cuts with the other conventional methods are well detailed in [16], [15]. Table I shows that the index is higher when we use our proposed method compared to the standard Graph-Cuts Method. Also, it can be seen that the mean value of the term  $\|R_{seg}\| \oplus \|R_{Gt}\|$  is very high compared to the proposed method. The reason why such difference between the two values is that the segmented region obtained using the graph-Cuts method contains parts from the trachea and the bronchus regions, confused with the lung parenchyma during the segmentation.

In the other hand, The mean value of the term  $\|R_{seg} \cap R_{Gt}\|$  is lower in the case of the standard graph cuts method compare to the proposed method.

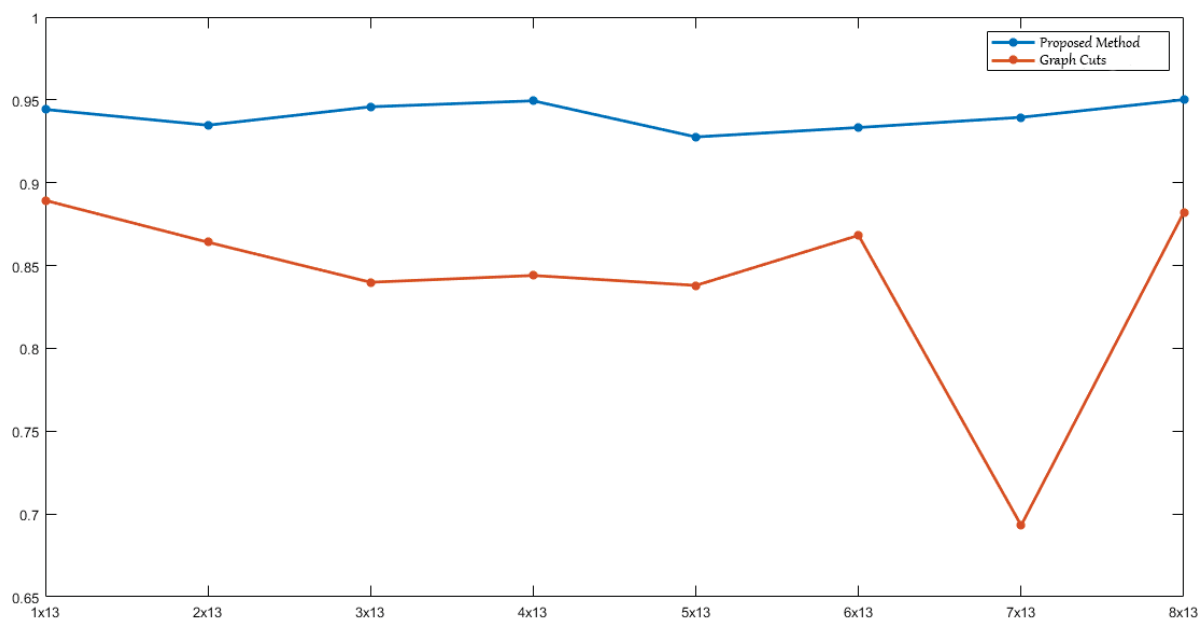


Fig. 1 The Mean Dice coefficient index value for all tested cases

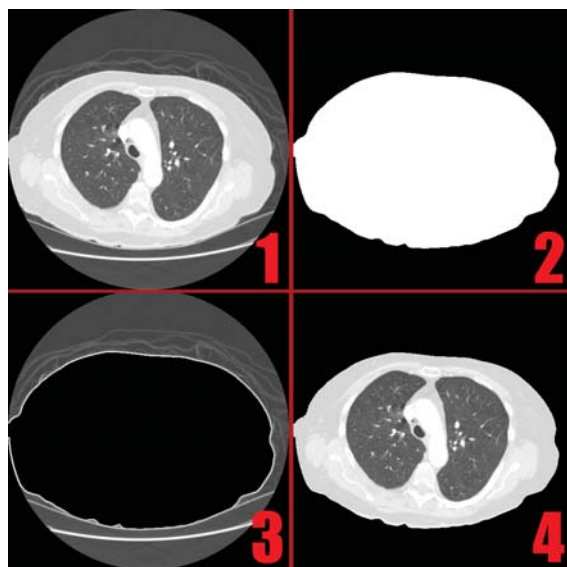


Fig. 2 (1) The original image (2) the obtained Ground Truth (3) the empty area O (4) the information Area

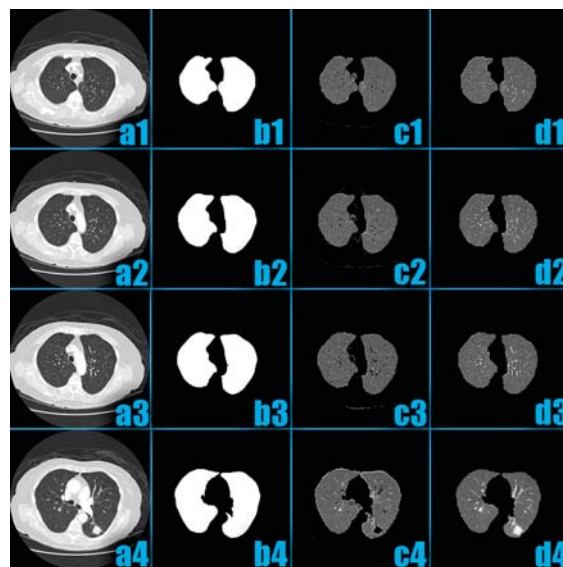


Fig. 3 The (a) block represents a sample of the DataSet numbered from 1 to 4. The block (b) represents the ground truth for the lung parenchyma performed manually by the Radiologist. The block (c) is the result of the Standard Graph-Cuts image segmentation while the result of the proposed method is figured in the block (d)

This is due to the high false positive rate in the case of the standard graph cuts compared to the proposed method.

Fig. 3 shows the experimentation results in which we compare our proposed method with the standard Graph-Cuts. The figure contains four columns. From the left to the right, each one represents the original image, the Ground Truth of the Lung parenchyma, the result segmentation using the Graph-Cuts and the Results of the proposed method respectively.

The 3<sup>rd</sup> column shows that the lung segmentation results contains parts of the trachea and the bronchus regions. Also, lesions such as nodules and parts of the blood vessels are

not segmented with the lung parenchyma. Differently, the 4<sup>th</sup> column shows an accurate segmentation of the proposed method, especially for lung nodules and blood vessels; with 0.9406 Dice coefficient index. The result of all tested cases can be shown in Fig. 1.

## V. CONCLUSIONS

In this work, we proposed an improved version of the Graph Cuts Based Lung CT image segmentation. The main subject of this research was to obtain an accurate segmentation of Lung



parenchyma in CT images, especially for pathological lungs. While other conventional methods need a post-processing to obtain satisfying results, our method performs Better Without any post-processing.

#### REFERENCES

- [1] C. A. Ridge, A. M. McErlean, and M. S. Ginsberg, "Epidemiology of lung cancer," in *Seminars in interventional radiology*, vol. 30, pp. 093–098, Thieme Medical Publishers, 2013.
- [2] C. E. DeSantis, C. C. Lin, A. B. Mariotto, R. L. Siegel, K. D. Stein, J. L. Kramer, R. Alteri, A. S. Robbins, and A. Jemal, "Cancer treatment and survivorship statistics, 2014," *CA: a cancer journal for clinicians*, vol. 64, no. 4, pp. 252–271, 2014.
- [3] L. Tsochatzidis, K. Zagoris, N. Arikidis, A. Karahaliou, L. Costaridou, and I. Pratikakis, "Computer-aided diagnosis of mammographic masses based on a supervised content-based image retrieval approach," *Pattern Recognition*, 2017.
- [4] J. won Cha, M. M. Farhangi, N. Dunlap, and A. Amini, "Volumetric analysis of respiratory gated whole lung and liver ct data with motion-constrained graph cuts segmentation," in *Engineering in Medicine and Biology Society (EMBC), 2017 39th Annual International Conference of the IEEE*, pp. 3405–3408, IEEE, 2017.
- [5] W. Zhang, X. Wang, P. Zhang, and J. Chen, "Global optimal hybrid geometric active contour for automated lung segmentation on ct images," *Computers in biology and medicine*, vol. 91, pp. 168–180, 2017.
- [6] P. P. Rebouças Filho, P. C. Cortez, A. C. da Silva Barros, V. H. C. Albuquerque, and J. M. R. Tavares, "Novel and powerful 3d adaptive crisp active contour method applied in the segmentation of ct lung images," *Medical image analysis*, vol. 35, pp. 503–516, 2017.
- [7] I. Sluimer, A. Schilham, M. Prokop, and B. van Ginneken, "Computer analysis of computed tomography scans of the lung: a survey," *IEEE transactions on medical imaging*, vol. 25, no. 4, pp. 385–405, 2006.
- [8] S. Hu, E. A. Hoffman, and J. M. Reinhardt, "Automatic lung segmentation for accurate quantitation of volumetric x-ray ct images," *IEEE transactions on medical imaging*, vol. 20, no. 6, pp. 490–498, 2001.
- [9] S. G. Armato and W. F. Sensakovic, "Automated lung segmentation for thoracic ct: Impact on computer-aided diagnosis1," *Academic Radiology*, vol. 11, no. 9, pp. 1011–1021, 2004.
- [10] D. Mahapatra, "Semi-supervised learning and graph cuts for consensus based medical image segmentation," *Pattern Recognition*, vol. 63, pp. 700–709, 2017.
- [11] W. Sun, X. Huang, T.-L. B. Tseng, and W. Qian, "Automatic lung nodule graph cuts segmentation with deep learning false positive reduction," in *SPIE Medical Imaging*, pp. 101343M–101343M, International Society for Optics and Photonics, 2017.
- [12] Y. Y. Boykov and M.-P. Jolly, "Interactive graph cuts for optimal boundary & region segmentation of objects in nd images," in *Computer Vision, 2001. ICCV 2001. Proceedings. Eighth IEEE International Conference on*, vol. 1, pp. 105–112, IEEE, 2001.
- [13] C. Rother, V. Kolmogorov, and A. Blake, "Grabcut: Interactive foreground extraction using iterated graph cuts," in *ACM transactions on graphics (TOG)*, vol. 23, pp. 309–314, ACM, 2004.
- [14] S. Vicente, V. Kolmogorov, and C. Rother, "Graph cut based image segmentation with connectivity priors," in *Computer vision and pattern recognition, 2008. CVPR 2008. IEEE conference on*, pp. 1–8, IEEE, 2008.
- [15] K. Nakagomi, A. Shimizu, H. Kobatake, M. Yakami, K. Fujimoto, and K. Togashi, "Multi-shape graph cuts with neighbor prior constraints and its application to lung segmentation from a chest ct volume," *Medical image analysis*, vol. 17, no. 1, pp. 62–77, 2013.
- [16] S. Dai, K. Lu, J. Dong, Y. Zhang, and Y. Chen, "A novel approach of lung segmentation on chest ct images using graph cuts," *Neurocomputing*, vol. 168, pp. 799–807, 2015.
- [17] S. G. Armato, G. McLennan, L. Bidaut, M. F. McNitt-Gray, C. R. Meyer, A. P. Reeves, B. Zhao, D. R. Aberle, C. I. Henschke, E. A. Hoffman, et al., "The lung image database consortium (lidc) and image database resource initiative (idri): a completed reference database of lung nodules on ct scans," *Medical physics*, vol. 38, no. 2, pp. 915–931, 2011.
- [18] B. N. Narayanan, R. C. Hardie, T. M. Kebede, and M. J. Sprague, "Optimized feature selection-based clustering approach for computer-aided detection of lung nodules in different modalities," *Pattern Analysis and Applications*, pp. 1–13, 2017.
- [19] A. Buades, B. Coll, and J.-M. Morel, "A review of image denoising algorithms, with a new one," *Multiscale Modeling & Simulation*, vol. 4, no. 2, pp. 490–530, 2005.
- [20] H. Jomaa, R. Mabrouk, N. Khelifa, and F. Morain-Nicolier, "Denoising of dynamic pet images using a multi-scale transform and non-local means filter," *Biomedical Signal Processing and Control*, vol. 41, pp. 69–80, 2018.
- [21] A. El Hassani and A. Majda, "Efficient image denoising method based on mathematical morphology reconstruction and the non-local means filter for the mri of the head," in *Information Science and Technology (CiSt), 2016 4th IEEE International Colloquium on*, pp. 422–427, IEEE, 2016.
- [22] N. Deo, *Graph theory with applications to engineering and computer science*. Courier Dover Publications, 2017.
- [23] H. Lin, C. Huang, W. Wang, J. Luo, X. Yang, and Y. Liu, "Measuring interobserver disagreement in rating diagnostic characteristics of pulmonary nodule using the lung imaging database consortium and image database resource initiative," *Academic Radiology*, vol. 24, no. 4, pp. 401–410, 2017.
- [24] S. Jeevakala et al., "Sharpening enhancement technique for mr images to enhance the segmentation," *Biomedical Signal Processing and Control*, vol. 41, pp. 21–30, 2018.